ORIGINAL ARTICLE

Steel based retrofitting interventions for existing masonry walls: a comparative numerical investigation

Mattia Zizi, Alessandro Vari, Piero Colajanni, Gianfranco De Matteis

Correspondence

Gianfranco De Matteis
Dept. of Architecture and Industrial Design
University of Campania "Luigi Vanvitelli"
Abbazia di San Lorenzo ad Septimum
81031 Aversa (Caserta), ITALY
Email: gianfranco.dematteis@unicampania.it

Abstract

Masonry buildings constitute a significant portion of the architectural heritage all over the world, also in regions affected by a high seismic hazard. Since this constructional material is characterized by lack of tensile strength, as well as small deformation capacity, masonry structures could result hugely damaged if shaken by seismic forces. In order to avoid collapses and reduce structural damage, innovative retrofitting interventions are necessary to improve the seismic behavior of masonry structures. In this context, steel-based techniques could be considered among the most suitable solutions. In fact, by using such a high-performant material, additional strength and ductility may be conferred to existing masonry structures. Based on these premises, the present paper focuses on a numerical investigation of two different retrofitting techniques: the CAM© system and the application of steel grids on both faces of a masonry wall. In particular, on the base of an experimental test carried out within the research project In.CAM.M.I.N.O. on an unreinforced masonry wall tested in condition of constant vertical force and horizontal loads, a reference FE Model has been calibrated in Abaqus by using a macro-modelling approach with a damage-plasticity material model for the masonry. Then, based on the reference model, the efficiency of the two systems has been investigated and compared by means of numerical analyses, in order to evaluate the strength and ductility increases obtainable by the application of the two retrofitting techniques.

Keywords

Steel-based Retrofitting, Seismic capacity improvement, Existing masonry structures, FEM analyses.

1 Introduction

Since the first half of 18th century, steel structural elements have been widely adopted in the construction field, even though mainly for secondary issues in case of structures (e.g. tie rods, connector elements, etc.) [1]. Moreover, considering the ease of use and the mechanical potentiality of such a material, also based on the important applications experienced in the last century, nowadays it is very clear that the use of steel to enhance the structural behaviour of existing constructions could be very profitable.

In the context of existing structures, particular attention has to be focused on masonry buildings, due to the strong necessity that they have to be retrofitted in order to guarantee sufficient performances, especially in case of seismic loads. To appreciate the scale of the problem, it is interesting to note that more than 70% of the total worldwide building heritage is made by masonry constructions [2]. Moreover, to further corroborate such an assumption, it is worth mentioning the large amount of masonry heritage that was damaged or even collapsed after the meaningful earthquakes occurred in the last decade in Italy (L'Aquila 2009, Emilia 2012 and Central-Italy 2016-2017) and all over the world (e.g. China 2008, Chile 2010, Nepal 2015, Mexico 2017 and Indonesia 2018).

The inadequacy of masonry structures in case of exceptional actions is mainly due to the mechanical characteristics of the base materials, and in particular to the lack of tensile strength and reduced deformation capacity. In addition, it should be considered that in most cases, buildings were realized to sustain gravitational loads only and were designed based on simple empirical design rules. Nowadays, according to the stringent code provisions in seismic areas, it is clear that they present strong structural deficiencies.

Masonry structures subjected to horizontal forces may exhibit two main failure modes: out-of-plane (Mode I) or in-plane (Mode II) mechanisms. If on the one hand Mode I collapses could be avoided by guaranteeing good wall-slab connections, as well as between orthogonal walls, on the other, Mode II failure modes develop when the strength of the structural element is overcame and shear or flexural crisis could occur.

Since the occurrence of Mode II mechanisms strongly depends on the strength of the existing materials, in the last decades, many research activities have been carried out with the aim to propose innovative retrofitting techniques for the in-plane seismic behaviour improvement of existing masonry walls. In particular, the good performances in terms of strength, ductility and stiffness achievable by means of steel-based applications, in addition to the possibility to use limited quantity of additional material, makes such retrofitting techniques very effective.

Many examples of steel-based applications on masonry structures can be found in in literature, both conventional and innovative. Among these, it is worth mentioning the use of reinforced plaster [3, 4], shotcrete [5, 6], RC jacketing [7, 8], and external reinforcement [9, 10]. According to previous studies, it has been stated that the use of external reinforcement could be considered as the most efficient steel-based retrofitting techniques, providing a notable increment of strength and ductility, as well as of energy dissipation capacity, in presence of horizontal loads [11].

Based on these premises, in the present paper two different steel-based external retrofitting techniques suitable for in-plane seismic behaviour improvement of masonry walls are examined. In particular, the CAM® system and the traditional steel grids are investigated by means of a numerical study, allowing to provide a comparison between the two techniques, whose suitability has been widely demonstrated in the past [12, 13, 14].

2 The reference numerical model

2.1 General

In this section, the implementation of the reference numerical model is presented. In particular, the FE Model has been calibrated on the basis of the evidences obtained from a previous experimental campaign, carried out as part of the framework of the In.CAM.M.I.N.O. research project.

2.2 The reference test

The considered reference test consisted in a Sheppard test on a masonry panel [15]. The test set-up provided a vertical compressive force of 200 kN applied on the top of the wall and a successive incremental horizontal load applied at its mid-height.

The tested specimen has been obtained from an existing retaining wall placed in the city of Messina and was characterized by a very poor masonry, with bad mechanical characteristics and arrangement, such as also demonstrated by preliminary characterization tests. The thickness and the total height of the panel was 0.55 and 2.15 meters, respectively, while the width was 1.10 meters.

In order to avoid rotations in the both top and bottom sections, as well as in the mid-height one, rigid elements have been introduced: a 50 centimetres high R.C. beam has been adopted for the upper side, while coupled UPN 200 with two transversal bolt (ϕ24) have been introduced in the mid-height and at the base of the panel. Moreover, four dywidag bars have been inserted between the downer and the upper rigid elements, in order to guarantee a correct transmission of the vertical load.

A picture of the set-up test is provided in Figure 1a, while further details concerning the experimental campaign can be found in Spinella et al. [13].

At the end of the experimental test, the specimen exhibited a typical diagonal shear failure with a different damage level for the two half-panels (Figure 1b).

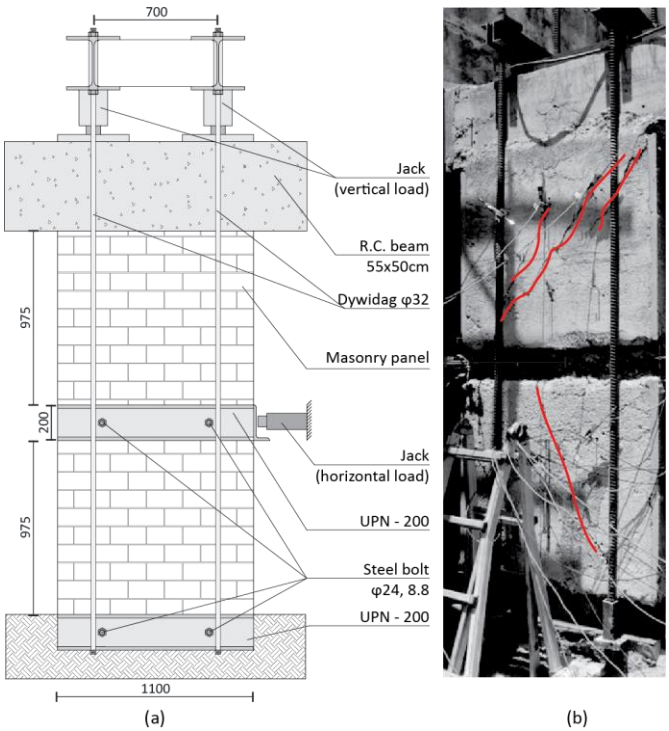

Figure 1 Set-up of the reference test

In particular, since the stiffness of the upper R.C. beam was significantly higher than the UPN system at the base, the upper half-panel absorbed a larger proportion of the horizontal load.

The force-displacement response returned by the test is provided in Figure 2. At the end of the test a maximum shear force and an ultimate displacement of approximatively 180 kN and 18 mm, respectively, were attained.

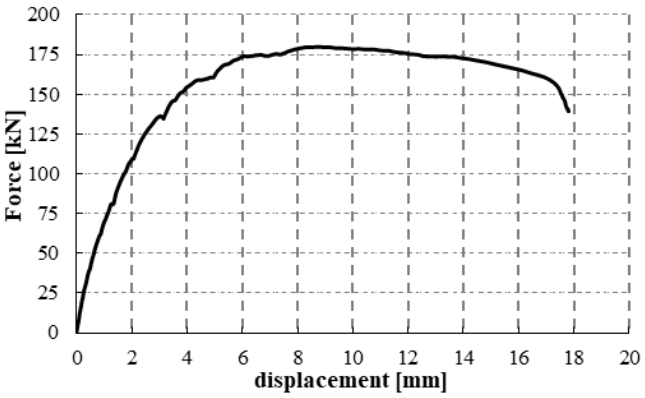

Figure 2 Force-displacement response of the reference experimental test

2.3 Numerical modelling

The response of the reference test has been simulated by means of a numerical analysis implemented in Abaqus/Standard solution. Three-dimensional elements with a mesh of 5 centimetres have been used for the panel modelling with 8 nodes and reduced integration elements (namely C3D8R). For the masonry, a macro-modelling approach has been adopted, which represents a very suitable tool to catch the global response of such a material typology.

In order to simulate the presence of the rigid beams, internal constraints have been introduced in the model. In particular, the base and the top nodes, as well as those of the mid-height section, have been rigidly linked to external reference points (RPs) by means of rigid bodies: in such a way both loads and external constraints applied to RPs are directly transferred to the panel.

Moreover, the presence of dywidag bars has been simulated by introducing axial springs, whose stiffness has been evaluated according to the dimension of the bars.

The analysis has been phased in two separate steps: in the first step the vertical load has been applied, while in the second one the horizontal force has been introduced by means of a displacement control.

It is worth noticing that in the real test, the vertical load was applied by imposing a tensile stress to the dywidag bars and therefore provoked a lift-up of the base section, rather than an infinitesimal downward movement of the upper side of the panel. This phenomenon provoked the aforementioned unexpected rotations of the base section.

Based on these considerations, the following external constraint conditions have been assumed for the analysis:

- For the upper RP, a total encastre has been adopted during both steps of the analysis;
- To the downer RP, the only vertical movements has been permitted during the first step of the analysis, while during the lateral load application all degrees of freedom were fixed with exception of the horizontal displacement and in-plane rotation. Moreover, a lateral spring with a stiffness of K=7.6 kN/mm accounting the possible infinitesimal movements of the bolts-UPN system has been introduced.

Hence, the vertical loads during the first step and an increasing horizontal displacement during the second one have been applied on the downer and middle-height reference nodes, respectively.

The masonry material has been modelled by using a plastic-damage material with a smeared approach, namely the Concrete Damage Plasticity, which is available in the library of Abaqus. The adopted material model was firstly conceived for concrete structures but it is also suitable for simulating the response of quasi-brittle material, such as masonry. In particular, it is based on the amendments introduced by Lee and Fenves [16] on the material model proposed by Lubliner et al. [17].

Table 1 Adopted parameters for the masonry modelling

Parameter	Value
Density [γ]	1900 kg/m^3
Young's Modulus [E]	633
Poisson's ratio [υ]	0.3
Dilation angle [ψ]	35°
Eccentricity	0.1
f_{c0}/f_{b0}	1.16
Kc	0.66
Compressive post-elastic behaviour	Parabola-rectangle
Compressive elastic strength [f_y]	0.3 MPa
Compressive ultimate strength [f_k]	1 MPa
Maximum compressive strain [ε_u]	3.5‰
Tensile post-elastic behaviour	Linear softening
Tensile strength [f_t]	0.23 MPa
Ultimate tensile displacement [u_{t0}]	2.5 mm

The parameters of the material model have been calibrated on basis of the results arisen from the preliminary characterization tests, which for the sake of brevity are not reported in this paper.

A summary of the adopted parameters is reported in Table 1.

2.4 Numerical results and definition of the reference model (URM_REF)

The numerical model resulted in a good agreement with the reference test. In particular, as it can be appreciated in Figure 3, the correspondence in terms of force-displacement curve between the numerical analysis (stated as URM) and the reference test is very good.

In fact, both initial stiffness and maximum shear strength are correctly captured by the numerical model, as well as the softening branch after the peak force.

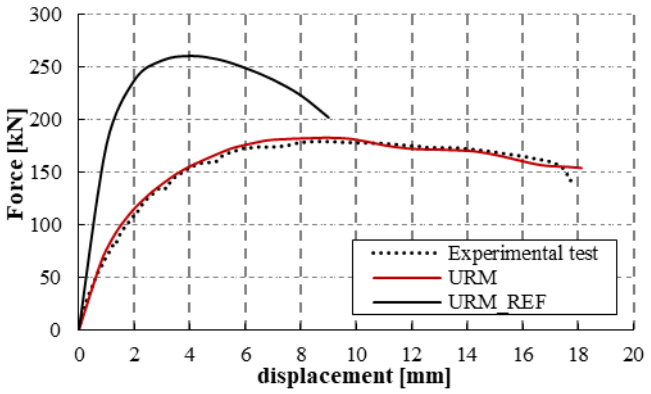

Figure 3 Results of the URM and REF numerical models: force-displacement curve in comparison with the reference experimental test

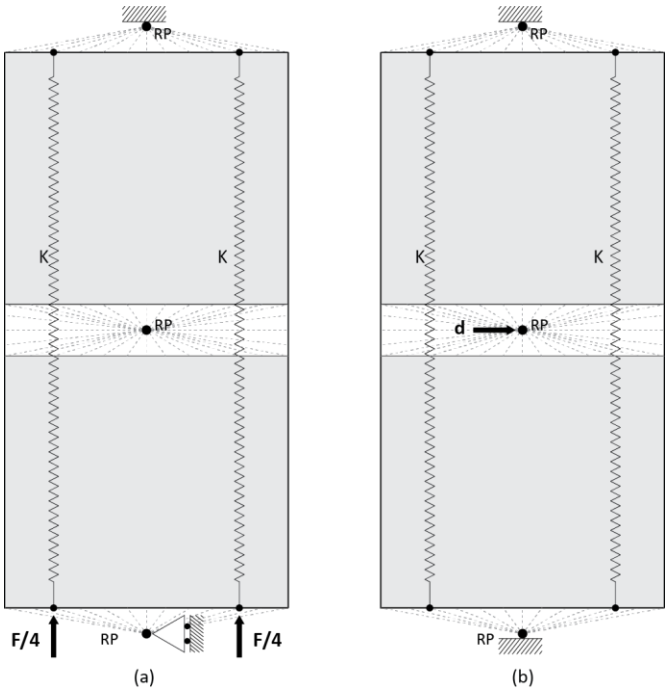

Figure 4 Boundary conditions (load and external constraints) and internal constraints of the URM_REF: (a) first step (vertical load) and (b) second step (horizontal displacement)

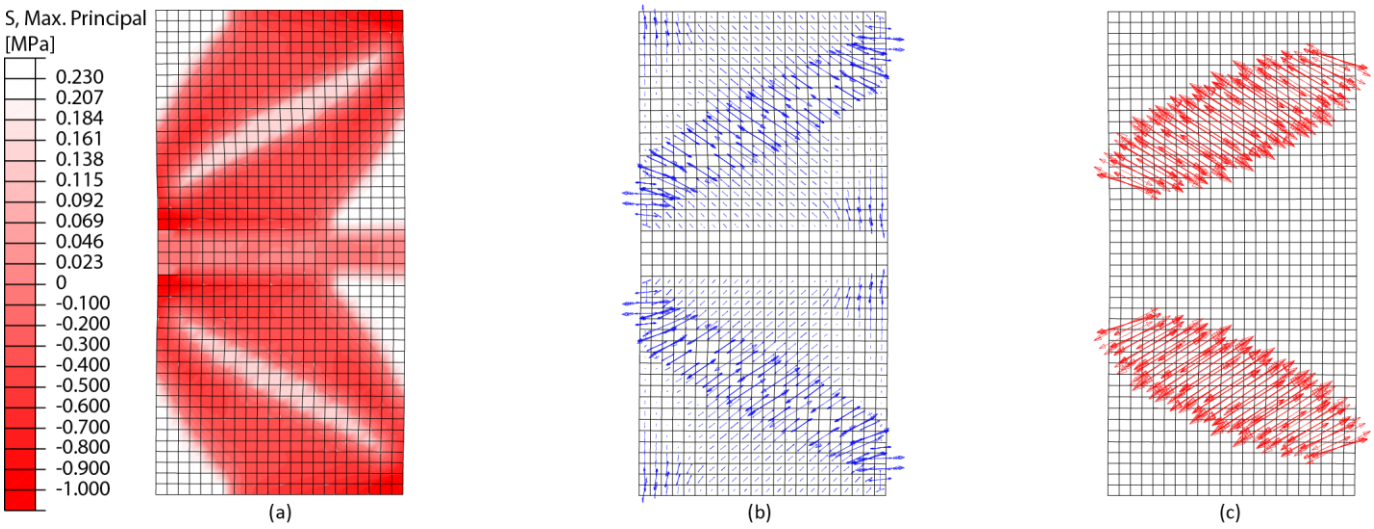

Figure 5 Stress trend (a), compressive (b) and tensile plastic strain (c) at the end of the URM_REF analysis (conventional failure point at a lateral displacement of 9 mm)

Once that the material behaviour and the set-up test have been faithfully reproduced, a new model has been implemented, which has been considered as reference for the aims of the present study (stated as URM_REF).

In particular, in the URM_REF the constraint conditions have been modified, in order to simulate the presence of perfectly rigid elements, both at top and bottom of masonry panel. Therefore, only vertical translation has been permitted to the bottom reference node during the application of the vertical load, while in the second step a fixed constraint condition has been introduced. Hence, also for this analysis, a total encastre has been assumed for the upper side of the wall during both steps.

The load conditions, as well as the internal constraints and axial springs, used in the new URM_REF, were the same of the previous analysis, with four springs put at the dywidag bar locations and rigid bodies in order to consider the presence of the rigid beams.

A schematization of the boundary condition and the internal constraints adopted for each phase of the URM_REF analysis is provided in Figure 4.

As it is was possible to predict, the URM_REF model exhibited a stiffer initial response, with a higher maximum lateral force (261 kN), although with less ductility and a steeper softening branch in the post-peak phase (Figure 3). The analysis was interrupted when a decreasing of the 20% of the maximum lateral force occurred, corresponding to a lateral displacement of 9 mm.

At the end of the analysis, the URM_REF revealed a failure mode typical of a shear collapse, with cracks along the diagonal and concentrations of compressive stresses in the corners, as shown in Figure 5.

3 The investigated retrofitting techniques

3.1 General

In the present Section the retrofitting techniques are described, namely the CAM® system and the traditional steel grids. In particular, detailed geometrical characteristics and implementing issues, as well as the mechanical principles at the base of their functionality, are provided.

3.2 The CAM® System

The CAM® system is an efficient steel-based technique for the structural enhancement of existing buildings. Its application is very versatile and results suitable for both reinforced concrete and masonry structures.

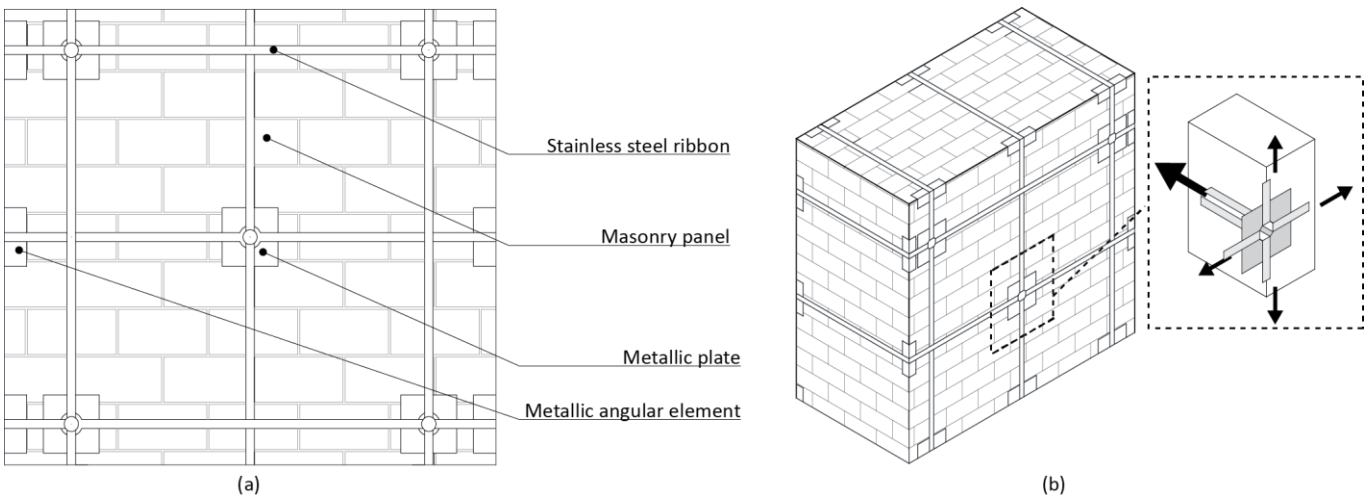

Figure 6 Example of application of the CAM® system: (a) frontal view and (b)axonometric view with particular of the functionality principle

The use of the CAM® system for masonry elements, such as columns or walls, consists in the introduction of a three-dimensional mesh made up of stainless steel ribbons of limited thickness (s≤1mm). The steel elements, which are pre-tensioned in order to provide a beneficial confinement effect to the existing material, lie directly on the external surfaces of the masonry and, in case of walls, pierce them throughout holes specifically realized.

In addition to the increment of the compressive state, which obviously prevents shear and flexural early failures, the first effect of the three-dimensional mesh is to act as drills and guarantee good transversal connections. In such a way, out-of-plane mechanisms, such as the desegregation of the material, which is typical in case of a poor masonry characterized by different layers, are avoided.

Moreover, the presence of steel elements guarantees a notable improvement of the seismic behaviour, providing additional strength and ductility, as well as compensating the stiffness degradation of the masonry in the post-elastic range.

An example of application of the CAM® system is schematically provided in Figure 6, where it is possible also to appreciate the presence of small metallic plates in correspondence of the holes and angular elements in the corner, which are introduced with the aim to avoid stress peaks in the base material.

In general, when the CAM ® system is applied on real buildings, its gable effects can be also exploited to guarantee a similar-box behaviour of existing buildings, avoiding the possibility to develop I Mode collapse mechanisms, such as overturning of walls.

Additional details about the CAM® system may be found in [12, 13, 18].

3.3 Steel grids

The alternative retrofitting techniques is based on the application on both faces of masonry panel of vertical and horizontal steel elements with a regular spacing, which are welded to each other in order to create a solid grid, and pasted on the masonry faces by means of a high-performance epoxy resin. When necessary, in order to guarantee a better connection and efficiency of the system steel plates, bolted to the masonry, can be introduced at the grid extremities.

Such a system, which has been already investigated by means of numerical analyses [14,19], is adopted mainly for the possibility to increase the system ductility and also the shear and the flexural strength of the base masonry panel. In particular, the above retrofitting system may be more efficient when it is anchored both at top and bottom edge of the masonry panel, namely to the foundations, inter-story beams and kerbs.

The main mechanical effect due to steel grids is that by introducing steel-mesh in the existing material, the stress trend and the failure modes could be favourably changed. In particular, when a masonry wall is simultaneously subjected to vertical and horizontal loads, a compressed strut is present, which, in presence of such a device, can be absorbed by horizontal and vertical forces, similarly to a multiple Ritter-Morsch model [20, 21].

Since this system could result rather invasive when applied to an entire building, its application is more suitable for few masonry walls. Therefore, differently from the CAM® system, it could be considered more appropriate for local interventions rather than for global interventions.

An example of application on a masonry wall is reported in Figure 7.

4 The numerical study

4.1 General

A numerical analysis has been carried out in order to compare the two investigated systems, as well as to verify their suitability in terms of structural performance.

In particular, based on the implemented URM_REF, two additional analyses have been implemented with the application of the both CAM® and steel grids systems, whose calibrations, develops and results are provided in this section.

4.2 Geometrical features of the retrofitted walls

For the definition of the geometrical characteristics of the studied

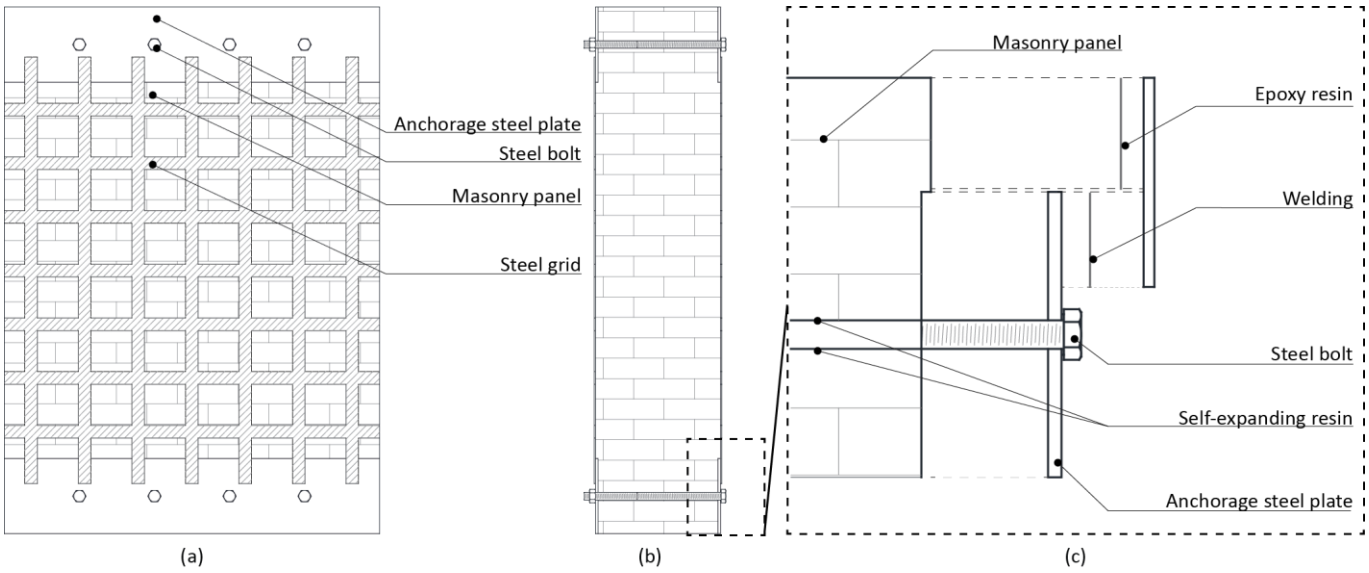

Figure 7 Example of application of steel grids: (a) frontal view, (b) transversal section and (c) anchorage particular

systems, reference to the aforementioned experimental campaign within the In.CAM.M.I.N.O. research project has been made [13]. In particular, in that context, a wall with the CAM® system composed by couples of 19 mm width and 1 mm thick stainless ribbons placed at a regular distance of 40 cm, was tested.

Hence, the same tested configuration has been adopted for the CAM® retrofitted wall.

It is worth noticing that such a test was interrupted before that the collapse of the masonry panel was reached, due to problem occurred during the experiment. Moreover, to avoid the occurrence of unexpected displacements and rotations, the base UPN profile was stiffened.

As far as the geometry of still grids is concerned, it has been defined considering the same steel quantity. Therefore, for the traditional steel grid system, steel elements with a width of 30 mm and a thickness of 2 mm have been adopted, while the pitch has been defined in order to obtain a regular vertical and horizontal spacing.

Hence, the retrofitted configurations shown in Figure 8a and 8b for the CAM® and steel grids systems, respectively, have been adopted in the numerical analyses.

A both top and bottom sides, as well as in the mid-height section, the presence of a rigid beam has been considered.

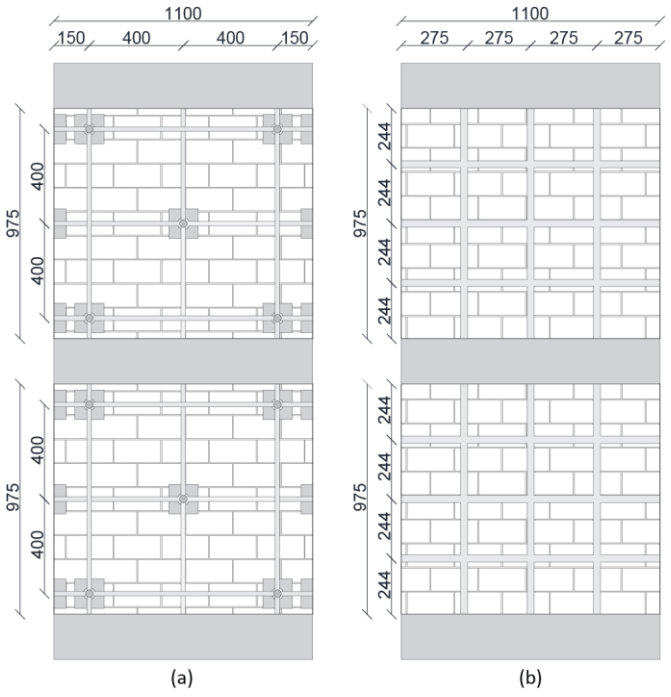

Figure 8 Geometrical configurations of the retrofitted walls: (a) CAM® system and (b) steel grids

4.3 Numerical modelling of the wall retrofitted with the CAM® system (RM_C)

The FE Model of the wall retrofitted with the CAM® system (RM_C) has been implemented on the basis of the URM_REF, by adopting the same boundary conditions. Therefore, since as aforementioned the base section was stiffened in the experimental test on the reinforced wall, the adoption of a perfect encastre at the base practically corresponds to the test at issue.

In order to allow, the passage of the stainless steel ribbons, holes in the masonry mesh have been introduced. The steel elements have been modelled by adopting shell elements with four nodes and reduced integration (CPSR4).

The overlapping of steel ribbons has been simulated by adopting a unique element with a thickness of 2 mm, for which a mesh width of 2 cm has been considered.

The pre-tension applied to the steel elements, which could be approximatively estimated at 200 MPa, has been simulated in the model by means of a thermal variation. At this aim, an *expansion* behaviour has been assumed for the material of the reinforcement elements, with a thermal coefficient of α_c=1.2·10^{-5} °C^{-1}. Therefore, an additional step, before the vertical load application, has been introduced in the analysis, in which the temperature of the stainless steel elements has been varied with a difference of ΔT=-80°.

The constitutive stress-strain relationship adopted for the stain steel is a typical bi-linear law with an Elastic Modulus E=212000 MPa, a yielding stress of f_y=317 MPa, an ultimate strength f_k=567 MPa and an ultimate strain ε_u=5.4%, as resulted by preliminary tests [13].

Moreover, also the CAM® elements have been rigidly linked to the references nodes, in order to simulate the perfect connection with the external beams.

Then, in order to simulate the presence of the small metallic plates close to the masonry holes typical of the CAM® system, additional rigid elements have been introduced, so to avoid stress peaks in the masonry.

The interaction between steel and masonry elements has been modelled by defining a *hard contact* in the normal direction and a *penalty* behaviour with a frictional coefficient of 0.3 in the tangential one.

A global view of the FE Model RM_C is shown in Figure 9a.

4.4 Numerical modelling of the wall retrofitted with the steel grids (RM_S)

As far as the numerical model of masonry wall with steel grids is concerned, for the steel element modelling, shell elements CPSR4 with a mesh of 2 cm have been adopted. The steel used for the reinforcement system is S235; a typical bi-linear law, with an Elastic Modulus E=210000 MPa, a yielding stress of f_y=235 MPa and an ultimate strength f_k=360 MPa, has been assumed.

The steel grid extremities have been added to the existing rigid bodies, namely in correspondence of the top, bottom and mid-height beams. It is worth mentioning that the welding connection adopted for real applications avoids significant stresses in the epoxy resin layers used for pasting steel to masonry, therefore perfect constraints, namely *surface ties*, have been introduced in the model in order to simulate their presence.

In general, the adopted boundary conditions, i.e. external constraint and loads, were the same of the previously described analysis.

A picture of the RM_S is provided in Figure 9b.

4.5 Analysis results

The analyses of the two retrofitted models were carried out considering the same load conditions of the URM_REF: constant vertical load of 200 kN and increasing horizontal displacement applied at

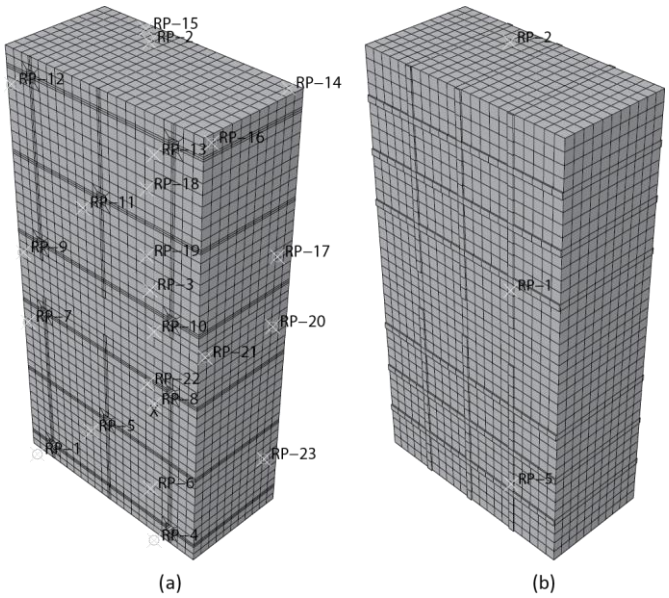

Figure 9 FE Models of the retrofitted walls: (a) RM-C and (b) RM_S

the mid-height up to failure. Since a displacement control has been adopted in the analyses, conventional failure points have been defined: the analyses were stopped when a decreasing of the 20% of the maximum lateral force occurred.

As it can be observed in Figure 10, where the obtained force-displacement curves are plotted in comparison with the URM_REF, at the end of the analyses, the reinforced walls revealed a significant improvement of structural behaviour, especially in terms of ductility.

In particular, the ultimate displacement (d_u) at the end of the analyses resulted 30 mm (+233%) and 19 mm (+110%) for the RM_C and RM_S, respectively.

Similarly, the maximum lateral forces (F_u) resulted equal to 272 kN (+4%) and 302kN (+16%) for the CAM® system and steel grids, respectively.

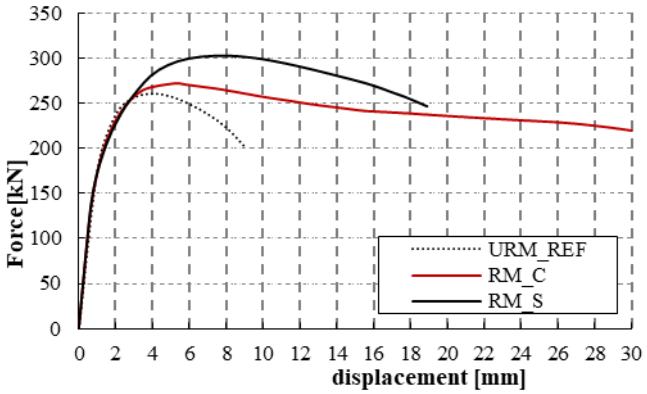

Figure 10 Results of the RM_C and RM_S numerical models: force-displacement curve in comparison with the URM_REF

On the contrary, the contribution of steel elements in terms of initial stiffening appeared to be negligible.

A summary of the ductility and strength increments are provided in Table 2.

Table 2 Efficiency of the investigated retrofitting techniques

Model	F_{max} [kN]	ΔF_{max} [%]	d_u [mm]	Δd_u [%]
URM_REF	261	---	9	---
RM_C	272	+4%	30	+233%
RM_S	302	+16%	19	+110%

In terms of global behaviour, it can be observed that the introduction of steel elements leads to postpone the occurrence of tensile stresses in the masonry material. This is clearly shown in Figure 11a and 12a, where for both retrofitted systems, at the conventional failure points, the tensile stress levels attained in the diagonals of

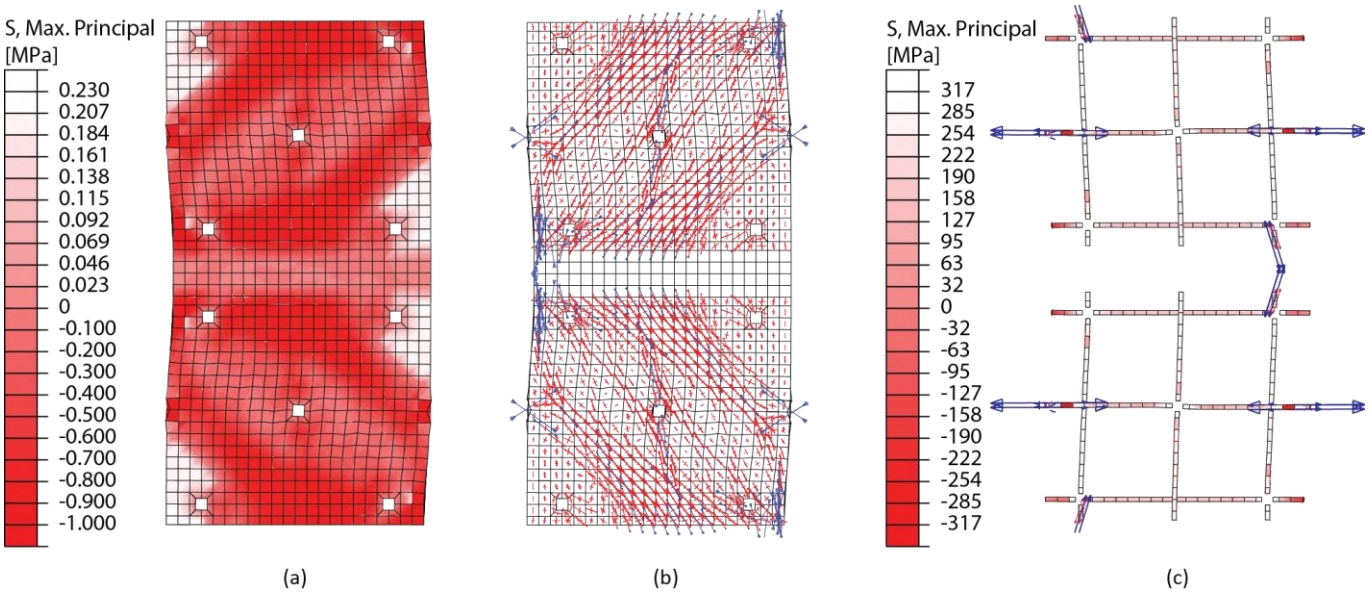

Figure 11 Analysis results of the retrofitted wall RM_C: (a) stress trend and (b) plastic strain of masonry and (c) stress trend and plastic strain at the failure point conventionally assumed at a lateral displacement of 30 mm (red and blue arrows are for tensile and compressive plastic strains, respectively).

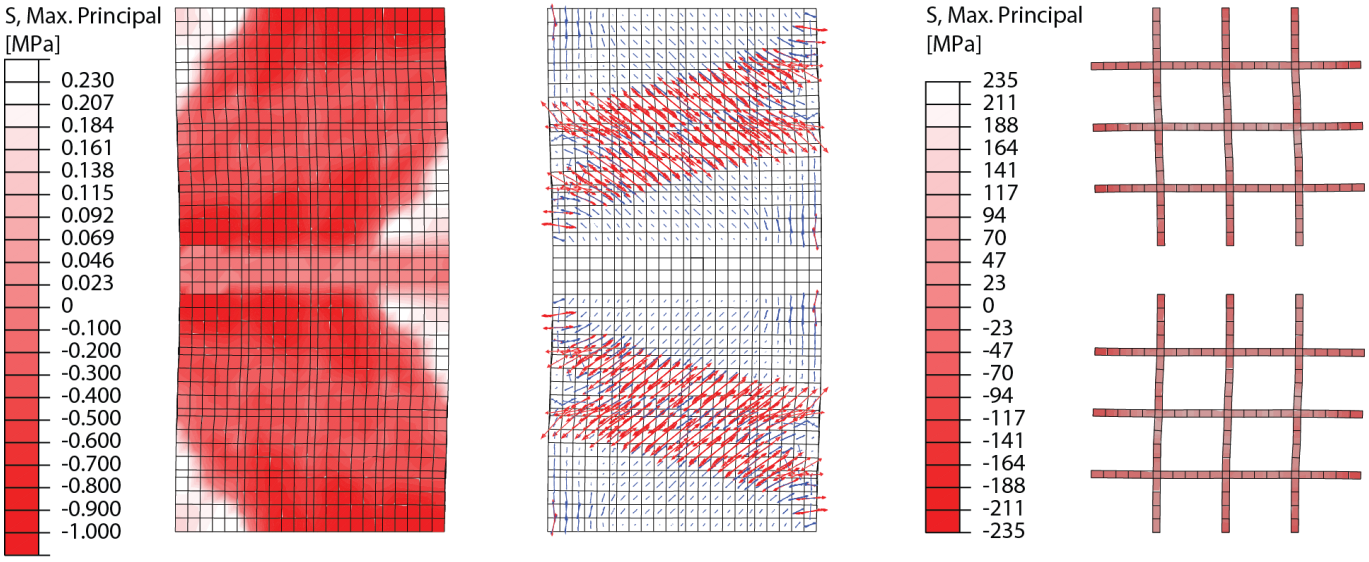

Figure 12 Analysis results of the retrofitted wall RM_S: (a) stress trend and (b) plastic strain of masonry and (c) stress trend and plastic strain at the failure point conventionally assumed at a lateral displacement of 30 mm (red and blue arrows are for tensile and compressive plastic strains, respectively).

the masonry panels were substantially lower than those registered for the URM_REF.

Moreover, the tensile plastic strains for retrofitted systems were more fairly distributed among the masonry area, avoiding concentration of crack along the diagonals (Figure 11b and 12b).

With regard to steel elements, the CAM® system provided a huge additional deformation capacity, by exploiting also to the ductility of the introduced material. In particular, as can be seen in Figure 11c, the stainless steel ribbons overcame their compressive or tensile yield stresses in several critical zones, such as the corners and the mid-height of the half-panels. As a consequence, a significant increment of ductility was provided to the masonry panel, despite the strength increase resulted almost negligible.

On the other hand, in case of traditional steel grid application, the panel returned a more accentuate hardening branch after the elastic limit, due to the fact that even at the failure point, the steel elements were still in the elastic field (Figure 12c).

The collapse mechanisms of the two retrofitted panels were due to a flexural failures for the CAM® and to a shear failure for the steel grids.

In particular, as it can be observed in Figure 11a, the presence of compressive plastic strain in the corners, as well as the higher ductility exhibited in the global response, are typical of a flexural crisis of the masonry, where also the post-elastic behaviour in compression is exploited. Such a behaviour is due to the additional confinement effect provided by the pre-tension applied on the stainless steel ribbons.

On the contrary, the adoption of steel grids led to a behaviour very similar to those exhibited by the unreinforced wall, since a shear failure with a diagonal cracking was reached at the end of the analysis, even though a significant increment of both strength and ductility was achieved.

5 Conclusions and future developments

In the present study a numerical investigation of two different steel-based reinforcement systems for existing masonry structures, namely the CAM® system and the application of steel grids on the both faces of masonry walls, has been proposed.

A reference numerical FEM Model has been implemented on the basis of a previous experimental test carried out on an existing unreinforced masonry wall.

Then, the two investigated steel-based reinforced systems have been introduced in the reference model and the improvement of the seismic behaviour in terms of strength and ductility has been evaluated.

The both systems revealed a significant improvement of the masonry wall behaviour in seismic load condition, especially in the post-peak phase. The presence of steel elements, indeed, provided to the unreinforced configuration a significant additional ductility and a not negligible increasing of shear capacity.

In the whole, the obtained results emphasised a good performance of both retrofitting systems, proving the suitability of such techniques for the structural enhancement of existing masonry structures.

6 Acknowledgements

The present study is part of a scholarship funded in the framework of the National Operational Program ESF-ESFR Research and In-novation (PON RI 2014-2020), Action I.1 related to Innovative Industrial Ph.D (Project Code – CUP - B25D18000010006) of which EDILCAM® Sistemi Srl is the industrial partner.

References

[1] Schulitz, H.C., Sobek, W., Habermann, K.J. (2000) *Atlante dell'acciaio*. Torino: UTET.

[2] Matthys, H., Noland, L. (1989). *Proceedings of an international seminar on evaluation, strengthening and retrofitting masonry buildings*. Colorado: TMS.

[3] Sheppard, P.; Tercelj, S. (1980) *The effect of repair and strengthening methods for masonry walls*. Proceedings of the 7th World Conference on Earthquake Engineering, September 8-13, Istanbul, Turkey. **6**, 255-262.

[4] Jabarov, M.; Kozharinov, S.; Lunyov, A. (1980) *Strengthening of*

damaged masonry by reinforced mortar layers. Proceedings of the 7th World Conference on Earthquake Engineering, September 8-13, 1980, Istanbul, Turkey. **6**, 73-80.

[5] Abrams, D. P.; Lynch, J. M. (2001) *Flexural behavior of retrofitted masonry piers*, KEERC-MAE Joint Seminar on Risk Mitigation for Regions of Moderate Seismicity. Illinois, USA.

[6] Kahn, L.F. (1984) *Shotcrete retrofit for unreinforced brick masonry*. Proceedings of the 8th World Conference on Earthquake Engineering, July 21-28, San Francisco, California, USA. **1** 583-590.

[7] Churilov, S.; Dumova-Jovanoska, E. (2013) *In-plane shear behaviour of unreinforced and jacketed brick masonry walls*. Soil Dynamics and Earthquake Engineering **50**, 85-105.

[8] Maheri, M.R.; Khajeheianb, M.K.; Vatanpourb, F. (2019) *In-plane seismic retrofitting of hollow concrete block masonry walls with RC layers*. Structures **20**, 425-436.

[9] Borri, A.; Castori, G.; Corradi, M.; Speranzini, E. (2011) *Shear behavior of unreinforced and reinforced masonry panels subjected to in situ diagonal compression tests*. Construction and Building Materials **25**(12), 4403-4414.

[10] Gattesco, N.; Amadio, C.; Bedon, C. (2015) *Experimental and numerical study on the shear behavior of stone masonry walls strengthened with GFRP reinforced mortar coating and steel-cord reinforced repointing*. Engineering Structures **90**,143-157.

[11] ElGawady, M.; Lestuzzi, P.; Badoux, M. (2004) *A review of conventional seismic retrofitting techniques for URM*. Proceedings of 13th International Brick and Block Masonry Conference, July 4-7, Amsterdam, Netherlands.

[12] Dolce, M.; Cacosso, A.; Ponzo, F. C.; Marnetto, R.; (2002). *New Technologies for the Structural Rehabilitation of Masonry Constructions: Concept, Experimental Validation and Application of the CAM System*. Seminar: "The Intervention On Built Heritage: Conservation and Rehabilitation Practices" (Invited lecture), October 2-4, Porto, Portugal.

[13] Spinella, N.; Colajanni, P.; Recupero, A. (2014). *Experimental in situ behaviour of unreinforced masonry elements retrofitted by pretensioned stainless steel ribbons*. Construction and Building Materials, **73**, 740-753.

[14] Zizi, M.; Campitiello, F.; Dogariu, A.; De Matteis, G.; (2017). *Cyclic response of brick-cement mortar masonry shear-walls retrofitted with steel grids*. Proceedings of 3rd International Conference on Protection of Historical Constructions PROHITECH 2017, July 12-15, Lisbon, Portugal.

[15] Turnsek, V.; Sheppard, P. F. (1980) *The shear and flexural resistance of masonry walls*. International research conference on earthquake engineering. June 30- July 3. Skopje, Bosnia-Herzegovina.

[16] Lubliner, J.; Oliver, J.; Oller, S.; Onate, E. (1989). *A plastic-damage model for concrete*. International Journal of Solids Structures, **25**, 299-326

[17] Lee, J.; Fenves, G. L. (1998). *Plastic-Damage Model for Cyclic Loading of Concrete Structures.* Journal of Engineering Mechanics, **124**(8), 892-900

[18] Spinella, N. *Push-over analysis of a rubble full-scale masonry wall reinforced with stainless steel ribbons*. Bull Earthquake Eng **17,** 497–518 (2019).

[19] Zizi, M.; Campitiello, F., De Matteis, G. (2017) *Risposta ciclica a taglio e criterio di dimensionamento di pannelli murarivrinforzati mediante graticci metallici*. In Proceedings of the XVII Convegno ANIDIS "l'Ingegneria Sismica in Italia". September 17-21, Pistoia, Italy.

[20] Mörsch, E. (1909) *Concrete-steel construction*. New York: McGraw-Hill Book Co.

[21] Ritter, W. (1899). *Die Bauweise Hennebique*. Zurich: Bauzeitun